

CrossMark  
click for updatesCite this: *J. Mater. Chem. C*, 2014, 2, 8492Received 25th June 2014  
Accepted 29th August 2014

DOI: 10.1039/c4tc01354a

www.rsc.org/MaterialsC

# Electrochemical synthesis of flat-[Ga<sub>13-x</sub>In<sub>x</sub>(μ<sub>3</sub>-OH)<sub>6</sub>(μ-OH)<sub>18</sub>(H<sub>2</sub>O)<sub>24</sub>(NO<sub>3</sub>)<sub>15</sub>] clusters as aqueous precursors for solution-processed semiconductors†

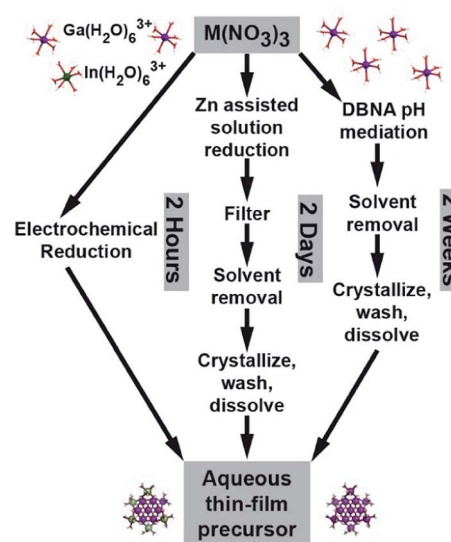
Matthew E. Carnes,\* Christopher C. Knutson, Athavan Nadarajah, Milton N. Jackson, Jr., Anna F. Oliveri, Kevin M. Norelli, Brandon M. Crockett, Sage R. Bauers, Hidekel A. Moreno-Luna, Benjamin N. Taber, Daniel J. Pacheco, Jarred Z. Olson, Kaylena R. Brevick, Claire E. Sheehan, Darren W. Johnson and Shannon W. Boettcher\*

Flat-[Ga<sub>13</sub>(μ<sub>3</sub>-OH)<sub>6</sub>(μ-OH)<sub>18</sub>(H<sub>2</sub>O)<sub>24</sub>](NO<sub>3</sub>)<sub>15</sub> (Ga<sub>13</sub>) and heterometallic [Ga<sub>13-x</sub>In<sub>x</sub>(μ<sub>3</sub>-OH)<sub>6</sub>(μ-OH)<sub>18</sub>(H<sub>2</sub>O)<sub>24</sub>](NO<sub>3</sub>)<sub>15</sub> (*x* = 5, 4) clusters were synthesized by the electrolysis of metal nitrate salt solutions to directly form, without purification, aqueous precursor inks for In<sub>x</sub>Ga<sub>13-x</sub>O<sub>y</sub> semiconducting films in <2 h. Raman spectroscopy and <sup>1</sup>H-NMR spectroscopy confirm the presence of [Ga<sub>13-x</sub>In<sub>x</sub>(μ<sub>3</sub>-OH)<sub>6</sub>(μ-OH)<sub>18</sub>(H<sub>2</sub>O)<sub>24</sub>(NO<sub>3</sub>)<sub>15</sub>] clusters. Bottom-gate thin-film transistors were fabricated using ~15 nm-thick Ga<sub>13-x</sub>In<sub>x</sub>O<sub>y</sub> films as the active channel layer, displaying turn-on voltages of -2 V, and on/off current ratios greater than 10<sup>6</sup>. The average channel mobility of the transistors fabricated from the cluster solutions generated by electrolysis was ~5 cm<sup>2</sup> V<sup>-1</sup> s<sup>-1</sup> which was more than twice that of transistors fabricated from control solutions with the simple nitrate salt precursors of ~2 cm<sup>2</sup> V<sup>-1</sup> s<sup>-1</sup>. Electrochemical cluster synthesis thus provides a simple and direct route to aqueous precursors for solution-processed inorganic electronics.

Thin film deposition using aqueous inorganic-cluster precursors provides an alternative to traditional vacuum processing techniques for thin-film deposition.<sup>1,2</sup> As one example, “flat” Group 13 [M<sub>13</sub>(μ<sub>3</sub>-OH)<sub>6</sub>(μ-OH)<sub>18</sub>(H<sub>2</sub>O)<sub>24</sub>(NO<sub>3</sub>)<sub>15</sub>], homo- and heterometallic clusters (Fig. 1) have been used to deposit high-performance semiconductor<sup>3</sup> and dielectric films.<sup>4</sup> Because of this, significant effort has been aimed at improving Group-13 cluster synthesis. Early syntheses took two weeks and used dibutyl nitrosamine (DBNA), a known carcinogen.<sup>3,5</sup> Wang *et al.* showed that the addition of Zn powder to acidic Al(NO<sub>3</sub>)<sub>3</sub> solutions results in condensation of [Al<sub>13</sub>(μ<sub>3</sub>-OH)<sub>6</sub>(μ-OH)<sub>18</sub>(H<sub>2</sub>O)<sub>24</sub>(NO<sub>3</sub>)<sub>15</sub>] (Al<sub>13</sub>) clusters *via* a gradual pH increase of the solution through nitrate reduction. The reaction is complete in approximately two days and the carcinogenic DBNA is no longer

needed.<sup>6</sup> A disadvantage to this method is that extensive purification is required to remove Zn<sup>2+</sup> from the precursor solution. The preferential solubility of zinc nitrate in alcohol is used to purify the clusters, as M<sub>13</sub> clusters are negligibly soluble in many organic solvents. In contrast, electrochemistry provides a direct mechanism to drive reduction reactions without the use of chemical reagents that must be later removed. Recently, both flat<sup>7</sup> and Keggin<sup>8</sup> Al<sub>13</sub> clusters have been electrochemically synthesized.

Here we report the electrochemical synthesis of [Ga<sub>13-x</sub>In<sub>x</sub>(μ<sub>3</sub>-OH)<sub>6</sub>(μ-OH)<sub>18</sub>(H<sub>2</sub>O)<sub>24</sub>]<sup>15+</sup> (*x* = 0, 4, 5) clusters and show that the aq. solutions obtained can be used, without purification, to deposit Ga<sub>13-x</sub>In<sub>x</sub>O<sub>y</sub> channel layers with good thin-film transistor (TFT) performance. The elimination of secondary reagents and purification steps is beneficial for mass production, sustainability, and cost. Films can be cast directly from the modified salt solutions, making this a direct method for

Fig. 1 Comparison of M<sub>13</sub> cluster synthesis routes.

Department of Chemistry & Biochemistry, the Materials Science Institute, the Center for Sustainable Materials Chemistry, University of Oregon, Eugene, Oregon 97403-1253, United States. E-mail: mec2105@gmail.com; swb@uoregon.edu

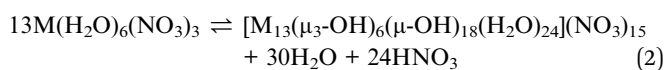
† Electronic supplementary information (ESI) available: Experimental details, NMR and EDX spectra. See DOI: 10.1039/c4tc01354a



obtaining various homo- and heterometallic Group 13 oxide thin films with a variety of applications.

The synthesis is performed in a two-compartment electrochemical cell comprised of a beaker housing (1) the Pt working electrode, a Ag/AgCl reference electrode, and a pH probe, and (2) a Pt counter electrode inside a medium-fritted glass tube that serves as a separate counter electrode compartment (Fig. S1†). Experimental details are provided in the ESI.† The applied working electrode potentials were chosen to be slightly negative of the reduction potential of the metal cations at the pH of interest as described by their Pourbaix diagrams.<sup>9</sup> Potentials of  $-1.00$  V vs. Ag/AgCl for Ga and  $-0.49$  V vs. Ag/AgCl for Ga–In mixtures were used to generate the desired products with the given apparatus. The voltage of  $-1.00$  V for aq. solutions of gallium nitrate caused a change in the luster of the Pt surface which could be seen by eye.<sup>10</sup> Yields of washed product show this plating results in a relatively small amount of Ga loss overall (<2%).

The primary mechanism of this reaction appears to be the removal of nitrate from the solution *via* its reduction to ammonium,  $\text{NO}_x$ , and other species. The removal of nitrate counter anions from the solution raises the pH of the solution by consuming protons as in, *e.g.*, eqn (1) and thus drives the formation of the cluster *via* LeChatelier's principle as it acts on the reaction as given in eqn (2).



Analysis of an air-dried aliquot of the crude reaction by  $^1\text{H-NMR}$  shows a prominent triplet peak with equal peak heights corresponding to the  $^1\text{H-}^{14}\text{N}$  coupling of ammonium ions centered at 7.1 ppm (ref. 11) (Fig. S3†). This indicates that nitrate is reduced to ammonium as a part of one pathway in which counterions are removed from solution and the pH is raised. Although the presence of ammonium ions indicates that nitrate reduction is involved in raising the pH of the cluster solution and forcing plating of the metal aqua species, it does not rule out other contributing mechanisms. We find that electrolysis at sufficiently high current results in evolution of a brown gas. This is likely due to the reduction of  $\text{NO}_3^-$  to  $\text{NO}_x$  gases.<sup>12</sup> We performed the electrochemical synthesis of  $\text{Ga}_{13}$  and  $\text{Ga}_{13-x}\text{In}_x$  mixed clusters at a constant applied voltage which was high enough to reduce small amounts of metal but low enough to prevent large losses of material to plating. We believe that some metal plating onto the electrode is important to condition the Pt toward nitrate reduction. Nitrate can undergo a number of reduction processes to form species including  $\text{N}_2\text{O}_4$ ,  $\text{HNO}_2$ ,  $\text{NO}$ , and  $\text{NH}_4^+$ . The standard reduction potentials are similar, between  $+0.8$ – $1.0$  V vs. NHE,<sup>13a</sup> and all much more positive than the hydrogen reduction potential. At a clean Pt electrode, however,  $\text{H}_2$  generation might be expected to dominate given the fast kinetics relative to nitrate reduction. We did not observe significant bubbles (that would be associated with  $\text{H}_2$  formation) on the Pt electrode surface. After Pt is

modified by Ga–In plating it likely becomes poisoned for hydrogen evolution and thus kinetically favors the nitrate reduction reaction.<sup>13b</sup> These data support the hypothesis that nitrate reduction is the predominant electrochemical reaction. Regardless of the cathode reaction, charge balance requires additional positively charged species (*e.g.*  $\text{In}(\text{H}_2\text{O})_6^{3+}$  or  $\text{Ga}(\text{H}_2\text{O})_6^{3+}$ ) to migrate from the counter electrode compartment into the working electrode compartment or negatively charged species (*e.g.*  $\text{NO}_3^-$ ) to migrate the opposite direction. Both migration processes serve to lower the nitrate-to-metal-ion ratio in the working-electrode-compartment film-precursor solution.

Proton NMR provides useful information for the identification and determination of the degree of substitution by indium in heterometallic clusters. Analysis of aq. inorganic clusters by  $^1\text{H-NMR}$  spectroscopy is traditionally challenging in protic solvents due to acidic proton exchange with the solvent. In most aprotic solvents, analysis of inorganic clusters by  $^1\text{H-NMR}$  spectroscopy is made difficult by the low solubility of highly-charged clusters. These obstacles are overcome by using  $d_6$ -DMSO, which allows for the detection of signals arising from water molecules and hydroxide bridges of the cluster. To confirm the presence of clusters, a portion of the electrochemically generated samples was air dried and then dissolved in  $d_6$ -DMSO. These samples were allowed to equilibrate overnight to ensure even DMSO exchange at the outer hydroxyl shell of the clusters.<sup>14</sup> The  $^1\text{H-NMR}$  spectra of the reduced  $\text{Ga}(\text{NO}_3)_3$  product is consistent with that of flat- $\text{Ga}_{13}$  clusters previously reported (Fig. S3†).<sup>15</sup>

Using  $^1\text{H-NMR}$ , we are able to distinguish between differently substituted heterometallic clusters once they have been dried and isolated. After equilibrating in  $d_6$ -DMSO for 24 h, the clusters for each Ga : In ratio gives rise to a distinctive spectrum with a clearly developed fingerprint region (ESI Fig. S4†). Although we can identify the Ga : In ratio from this signature, we are still unable to distinguish between positional isomers of the In at the exterior of the clusters. Crystals were grown of each of the isomers independently and their spectra taken to calibrate the results.<sup>16</sup> The  $^1\text{H-NMR}$  spectra obtained for the product of the mixed metal nitrate reduction, starting with a 6 : 7 ratio of Ga to In, is consistent with the  $\text{Ga}_9\text{In}_4$  cluster synthesized independently (ESI Fig. S4†). After washing the product of the electrochemical reaction with isopropanol, this product appears to have exchanged some of the external metal ions to form  $\text{Ga}_8\text{In}_5$  clusters as is evident by the change in their distinctive  $^1\text{H-NMR}$  spectra. This suggests that the clusters may be dynamic in the presence of the washing solvent and that In readily substitutes for Ga within the cluster (Fig. 2). Exchange of In atoms around flat  $\text{M}_{13}$  has recently been observed in solution to be a reversible, equilibrium process.<sup>16</sup>

We find evidence for  $\text{M}_{13}$  species forming with fewer reducing equivalents than that reported for the Zn-based synthesis of  $[\text{Al}_{13}(\mu_3\text{-OH})_6(\mu\text{-OH})_{18}(\text{H}_2\text{O})_{24}(\text{NO}_3)_{15}]^{6a}$ .  $\text{Ga}_{13}$  clusters are observed after passing a cathodic charge of 0.7–0.8 electrons per Ga, and 0.4–0.5 electrons per metal in the case of the  $\text{Ga}_{13-x}\text{In}_x$  clusters. The Zn-based synthesis of  $\text{Al}_{13}$  used 1.0 reducing equivalents per Al (1 : 2 Zn : Al as Zn is a  $2e^-$



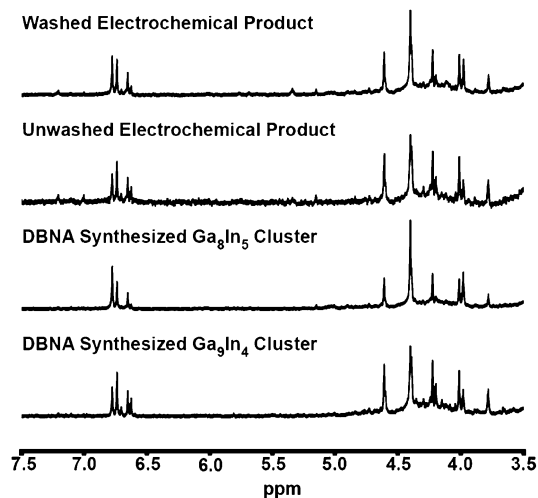


Fig. 2  $^1\text{H-NMR}$  ( $d_6$ -DMSO) spectra of washed and unwashed precipitated cluster products from DBNA and electrochemical syntheses. Based on comparison to the DBNA-derived control samples, the unwashed electrochemical product is assigned the composition  $\text{Ga}_9\text{In}_4$ , while the washed electrochemical product is assigned the composition  $\text{Ga}_8\text{In}_5$ .

reductant). The synthesis of a related  $\text{Sc}_2$  cluster used 0.75 reducing equivalents per Sc.<sup>6b</sup> Our hypothesis to explain such behavior is that if hydroxyl-bridged metal cluster formation is under equilibrium control, not all of the excess nitrate counterions need to be consumed for clusters to form. Our analysis does not however exclude the possibility that the reaction does not go to completion under the conditions used. Nitrate ions can also be effectively removed from association with the growing clusters by counterbalancing the positive charge associated with newly formed ammonium ions, leaving this new ammonium nitrate salt in solution but allowing ions to diffuse away from clustering species.

Raman spectroscopy is also useful for identifying  $\text{M}_{13}$  clusters.<sup>17</sup> The Raman spectra of aliquots from the electrochemical synthesis agree with previous reports of  $\text{Ga}_{13}$  clusters, highlighted by the  $\nu_1$  Ga–O symmetric stretch, or breathing mode at  $464 \pm 1 \text{ cm}^{-1}$  (Fig. 3).<sup>17</sup> The Raman spectra of the structurally analogous  $\text{Ga}_{13-x}\text{In}_x$  cluster reveal similar vibrational features to those observed in  $\text{Ga}_{13}$  clusters, with the  $\nu_1$  breathing mode slightly red-shifted to  $449 \pm 1 \text{ cm}^{-1}$ . This shift is consistent with the substitution of the larger In for Ga, and with the observed difference between the vibrational modes of In and Ga hexa-aqua salts (Fig. 3).

The class of flat  $\text{M}_{13}$  Group 13 clusters prepared previously have been shown to be effective precursors for high-quality thin films.<sup>3,4</sup> In this study, aq. cluster-containing solutions with an In : Ga ratio of 6 : 7 produced by the electrochemical synthesis were directly spin-cast onto thermally grown  $\text{SiO}_2$  on Si wafers and annealed at  $550 \text{ }^\circ\text{C}$ . This process circumvents the recrystallization step and the need to wash and dissolve the solid products in another solvent, thus reducing the time and solvent needed for synthesis. Heterometallic clusters were used to generate channel layers within TFTs. A TEM image of a device cross-section confirms the uniform morphology of thin films

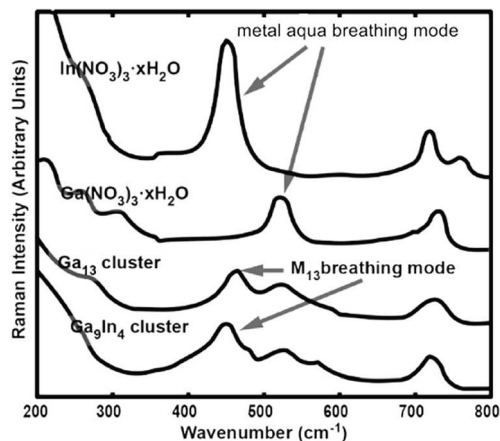


Fig. 3 Solid-state Raman spectra of nitrate salts and electrochemically generated cluster samples. Spectra for cluster compounds were collected on a single crystal using a Raman microscope and are largely free of metal nitrate impurities. Note the red-shift in the  $\nu_1$  breathing mode center for the In-substituted cluster ( $449 \pm 1 \text{ cm}^{-1}$ ) when compared to that for the Ga cluster ( $464 \pm 1 \text{ cm}^{-1}$ ). The uncertainties given are associated with the error in fitting the peak center.

processed from the electrochemically-synthesized precursor (Fig. 4a). EDX measurements of the films (Fig. S5<sup>†</sup>) confirmed the presence of both In and Ga in the films.

Fig. 4b–d show the device properties of the heterometallic cluster channel layer in TFTs processed from the electrochemically generated cluster solutions and compares them to those made using a starting nitrate salt solution. The devices derived

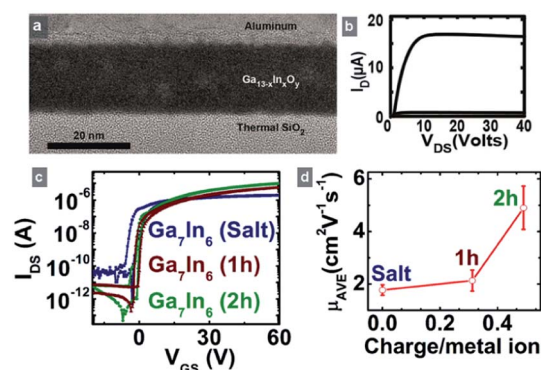


Fig. 4 (a) Transmission electron microscopy image demonstrating the uniform morphology of thin films processed from the electrochemically-synthesized precursor. (b) Average transfer curve compiled from five bottom-gate TFTs processed using the electrochemically synthesized  $\text{Ga}_{13-x}\text{In}_x$  heterometallic clusters to generate channel layers. (c) Representative transfer plots for  $550 \text{ }^\circ\text{C}$  air-annealed  $\text{Ga}_{13-x}\text{In}_x\text{O}_y$  films created using the electrochemically synthesized  $\text{Ga}_{13-x}\text{In}_x$  heterometallic cluster and starting salt solution precursors. (d) Average channel mobility determined at  $V_{\text{GS}} = 40 \text{ V}$  for films made at various electrolyzed time intervals (and thus different average numbers of electrons passed into the solution per metal ion). Device performance is increased with longer electrolysis, consistent with removal of nitrate and formation of clusters. The devices consist of the following structures: Al/Si (p+)/ $\text{SiO}_2$  (100 nm)/ $\text{Ga}_{13-x}\text{In}_x\text{O}_y$  (15 nm)/Al, length =  $150 \text{ }\mu\text{m}$ , width =  $1000 \text{ }\mu\text{m}$ , and  $V_{\text{DS}} = 0.1 \text{ V}$  ( $V_{\text{DS}}$  = drain source voltage;  $V_{\text{GS}}$  = gate source voltage;  $I_{\text{D}}$  = drain current).





from electrochemically-synthesized precursors are comparable to previously reported devices using DBNA-derived precursors.<sup>3</sup> Devices obtained from cluster precursors show on-to-off current ratios of greater than  $10^6$  and turn-on voltages near  $-2$  V whereas the devices made from starting salt solution show slightly negative turn-on voltages near  $-3$  V and on-to-off ratios greater than  $10^5$  (Fig. 4c).

The average channel mobility of cluster films are greater than those obtained from starting salt solution films by at least a factor of two (Fig. 4d). These values for mobility were calculated by the method of Wager *et al.* and should be considered the average mobility of the accumulated charge in the channel.<sup>18</sup> Compared to the mixed salt solutions of  $\text{In}(\text{NO}_3)_3$  and  $\text{Ga}(\text{NO}_3)_3$ , the  $\text{Ga}_{13-x}\text{In}_x$  clusters have fewer nitrate counter ions per active metal because the nitrates are consumed electrochemically during the cluster synthesis. This decrease in nitrate concentration drives olation and preorganization of the metal hydroxides into clusters.<sup>19</sup> Because nitrates must be removed during the annealing step to give an oxide thin film, we attribute the enhanced performance of the electrolyzed solution to reduced porosity in the final semiconductor channel that would be caused by decomposing counter ions.

Although the goal of this work is to show the new electrochemical synthesis route yields cluster precursors whose TFT performance is similar to clusters made by conventional methods, it is also useful to compare the performance to other solution-derived oxide thin films. Kim *et al.* reported the use of “combustion processing” to deposit related In–Zn–O films at temperatures as low as  $200$  °C from methoxyethanol solutions.<sup>20a</sup> Composition-optimized  $\text{In}_{0.7}\text{Zn}_{0.3}\text{O}_{1.35}$  devices fabricated with a  $\text{SiO}_2$  gate dielectric (as is done here) had saturation mobilities ( $\mu_{\text{sat}}$ ) of  $10 \text{ cm}^2 \text{ V}^{-1} \text{ s}^{-1}$  after annealing at  $400$  °C. Hwang *et al.* reported  $\mu_{\text{sat}}$  of  $8 \text{ cm}^2 \text{ V}^{-1} \text{ s}^{-1}$  for  $\text{In}_{0.7}\text{Zn}_{0.3}\text{O}_{1.35}$  after annealing at  $300$  °C when  $\text{Zn}(\text{NO}_3)_2$  and  $\text{In}(\text{NO}_3)_3$  were deposited from an aqueous solution.<sup>20b</sup> The  $\text{In}_{0.46}\text{Ga}_{0.53}\text{O}_{1.5}$  studied here had average channel mobilities of  $5 \text{ cm}^2 \text{ V}^{-1} \text{ s}^{-1}$ . Studies of vapor-deposited films show that mobility increases sharply with higher In concentration.<sup>20c</sup> Increasing the In : Ga ratio in the clusters would be expected to further increase TFT performance. Alternative gate dielectrics (*e.g.* amorphous alumina<sup>20d</sup>), and surface/interface passivation layers,<sup>21</sup> also dramatically improve the TFT performance of films made from other solution precursors. These strategies can directly be used to improve the performance of the cluster precursors reported here.

In summary, an alternate synthetic method is reported for the synthesis of flat homo- and heterometallic Group 13 cluster precursor solutions that can be directly used in the fabrication of thin-film transistors. This new method reduces the processing time to generate  $\text{M}_{13}$  cluster solutions from two days to two hours. The synthesis is carried out electrochemically so as to reduce protons and nitrate ions in a controlled fashion. Heterometallic clusters synthesized using this method are functionally similar in transistor applications to previously synthesized and characterized clusters.<sup>3</sup> These films are capable of being spin-cast directly from unpurified reaction solutions into high-quality thin films. The films are dense, smooth, and

processable at relatively moderate temperatures under ambient atmospheric conditions. This reagent-free, electrochemical synthesis may also find application in future mechanistic studies of cluster formation and speciation.

## Acknowledgements

This work was funded by National Science Foundation (NSF) grant CHE-1102637 and was the result of a research-based immersion course in cluster/film chemistry developed by the NSF Center for Sustainable Materials Chemistry. We acknowledge Jeffrey Ditto and Josh Razink for assistance in electron beam imaging. The CAMCOR shared instrument facilities are supported by grants from the W.M Keck Foundation, the M.J. Murdock Charitable Trust, ONAMI, the Air Force Research Laboratory (FA8650-05-1-5041), NSF (0923577 and 0421086) and the University of Oregon. SWB acknowledges support from the Research Corporation for Science Advancement as a Cottrell Scholar.

## Notes and references

- (a) K. Jiang, A. Zakutayev, J. Stowers, M. D. Anderson, J. Tate, D. H. McIntyre, D. C. Johnson and D. A. Keszler, *Solid State Sci.*, 2009, **11**, 1692–1699; (b) K. Jiang, J. T. Anderson, K. Hoshino, D. Li, J. F. Wager and D. A. Keszler, *Chem. Mater.*, 2011, **23**, 945–952; (c) S. T. Meyers, J. T. Anderson, D. Hong, C. M. Hung, J. F. Wager and D. A. Keszler, *Chem. Mater.*, 2007, **19**, 4023–4029; (d) S. T. Meyers, J. T. Anderson, C. M. Hung, J. Thompson, J. F. Wager and D. A. Keszler, *J. Am. Chem. Soc.*, 2008, **130**, 17603–17609; (e) J. T. Anderson, C. L. Munsee, C. M. Hung, T. M. Phung, G. S. Herman, D. C. Johnson, J. F. Wager and D. A. Keszler, *Adv. Funct. Mater.*, 2007, **17**, 2117–2124; (f) M. Alemayehu, J. E. Davis, M. Jackson, B. Lessig, L. Smith, J. D. Sumega, C. Knutson, M. Beekman, D. C. Johnson and D. A. Keszler, *Solid State Sci.*, 2011, **13**, 2037–2040; (g) A. Nadarajah, M. E. Carnes, M. G. Kast, D. W. Johnson and S. W. Boettcher, *Chem. Mater.*, 2013, **25**, 4080.
- (a) R. Murugavel, M. G. Walawalkar, M. Dan, H. W. Roesky and C. N. R. Rao, *Acc. Chem. Res.*, 2004, **37**, 763–774; (b) K. L. Furdala and T. D. Tilley, *J. Am. Chem. Soc.*, 2001, **123**, 10133–10134; (c) P. Sekar, E. C. Greyson, J. E. Barton and T. W. Odom, *J. Am. Chem. Soc.*, 2005, **127**, 2054–2055; (d) H. S. Kim, P. D. Byrne, A. Facchetti and T. J. Marks, *J. Am. Chem. Soc.*, 2008, **130**, 12580–12581.
- Z. L. Mensinger, J. T. Gatlin, S. T. Meyers, L. N. Zakharov, D. A. Keszler and D. W. Johnson, *Angew. Chem., Int. Ed.*, 2008, **47**, 9484–9486.
- S. W. Smith, W. Wang, D. A. Keszler and J. F. Conley Jr, *J. Vac. Sci. Technol., A*, 2014, **32**, 041501.
- (a) J. T. Gatlin, Z. L. Mensinger, L. N. Zakharov, D. Macinnes and D. W. Johnson, *Inorg. Chem.*, 2008, **47**, 1267–1269; (b) Z. L. Mensinger, W. Wang, D. A. Keszler and D. W. Johnson, *Chem. Soc. Rev.*, 2012, **41**, 1019–1030.
- (a) W. Wang, K. M. Wentz, S. E. Hayes, D. W. Johnson and D. A. Keszler, *Inorg. Chem.*, 2011, **50**, 4683–4685; (b)



- W. Wang, I. Y. Chang, L. Zakharov, P. H.-Y. Cheong and D. A. Keszler, *Inorg. Chem.*, 2013, **52**, 1807–1811.
- 7 W. Wang, W. Liu, I.-Y. Chang, L. A. Wills, L. N. Zakharov, S. W. Boettcher, P. H.-Y. Cheong, C. Fang and D. A. Keszler, *Proc. Natl. Acad. Sci. U. S. A.*, 2013, **110**, 18397.
- 8 C. Hu, H. Liu and J. Qu, *Colloids Surf., A*, 2005, **260**, 109–117.
- 9 M. Pourbaix, *Atlas of electrochemical equilibria in aqueous solutions*, National Association of Corrosion Engineers, 2nd English edn, Houston, 1974.
- 10 W. M. Saltman and N. H. Nachtrieb, *J. Electrochem. Soc.*, 1953, **100**, 126–130.
- 11 E. Pretsch, P. Bühlmann and M. Badertscher, *Structure Determination of Organic Compounds: Tables of Spectral Data*, 4th edn, Springer-Verlag, Berlin, 2009.
- 12 M. C. P. M. da Cunha, J. P. I. De Souza and F. C. Nart, *Langmuir*, 2000, **16**, 771–777.
- 13 (a) *Standard Potentials in Aqueous Solutions*, A. J. Bard, R. Parsons and J. Jordan, ed. International Union of Pure and Applied Chemistry, 1985; (b) T. Mahle, Metallic and bimetallic catalysts for electrochemical reduction of problematic aqueous anions, *Masters Thesis*, University of Illinois, Urbana-Champaign, 2012.
- 14 Samples are prepared for NMR by dissolving the sample in  $d_6$ -DMSO and allowing them to set for 24 h. Before that time the spectra is too complicated to analyze. Slow exchange with the solvent with the external waters of the cluster eventually results in a more simplified spectrum with a distinct fingerprint region. Fig. S4 in the ESI† shows how this fingerprint region changes as a function of In substitution within crystallographically confirmed  $Ga_{13-x}In_x$  clusters.
- 15 A. F. Oliveri, M. E. Carnes, M. M. Baseman, E. K. Richman, J. E. Hutchison and D. W. Johnson, *Angew. Chem., Int. Ed.*, 2012, **51**, 10992–10996.
- 16 M. K. Kamunde-Devonish, M. N. Jackson, Jr, Z. L. Mensinger, L. N. Zakharov and D. W. Johnson, *Inorg. Chem.*, 2014, **53**(14), 7101–7105.
- 17 M. N. Jackson, Jr, L. A. Wills, I.-Y. Chang, M. E. Carnes, L. Scatena, P. H.-Y. Cheong and D. W. Johnson, *Inorg. Chem.*, 2013, **52**, 6187–6192.
- 18 D. Hong, G. Yerubandi, H. Q. Chiang, M. C. Spiegelberg and J. F. Wager, *Crit. Rev. Solid State Mater. Sci.*, 2008, **33**, 101–132.
- 19 M. Henry; J. P. Jolivet and J. Livage, *Aqueous Chemistry of Metal Cations: Hydrolysis, Condensation and Complexation, Structure and Bonding*, Springer-Verlag, Berlin, 1992, vol. 77.
- 20 (a) M.-G. Kim, M. G. Kanatzidis, A. Facchetti and T. J. Marks, *Nat. Mater.*, 2011, **10**, 382; (b) Y. H. Hwang, J.-S. Seo, J. M. Yun, H. Park, S. Yang, S.-H. K. Park and B.-S. Bae, *NPG Asia Mater.*, 2013, **5**, e45; (c) T. Kamiya and H. Hosono, *NPG Asia Mater.*, 2010, **2**, 15.
- 21 (a) Y. S. Rim, H. Chen, X. Kou, H.-S. Duan, H. Zhou, M. Cai, H. J. Kim and Y. Yang, *Adv. Mater.*, 2014, **26**, 4273; (b) R. A. Street, T. N. Ng, R. A. Lujan, I. Son, M. Smith, S. Kim, T. Lee, Y. Moon and S. Cho, *ACS Appl. Mater. Interfaces*, 2014, **6**, 4428.

